

The TESS Triple-9 Catalog: 999 uniformly vetted exoplanet candidates

Luca Cacciapuoti¹,^{1,2,3}★ Veselin B. Kostov,^{4,5} Marc Kuchner,⁴ Elisa V. Quintana,⁴ Knicole D. Colón,⁴ Jonathan Brande¹,⁶ Susan E. Mullally,⁷ Quadry Chance,⁸ Jessie L. Christiansen,⁹ John P. Ahlers,¹⁰ Marco Z. Di Fraia¹,^{11,12} Hugo A. Durantini Luca,^{12,13} Riccardo M. Ienco,^{3,12} Francesco Gallo,^{3,12} Lucas T. de Lima,^{12,14} Michiharu Hyogo,^{12,15} Marc Andrés-Carcasona¹,^{12,16} Aline U. Fornear,¹² Julien S. de Lambilly¹,¹² Ryan Salik,^{12,17} John M. Yablonsky,¹² Shaun Wallace¹⁸ and Sovan Acharya^{12,19}

¹European Southern Observatory, Karl-Schwarzschild-Strasse 2, D-85748 Garching bei Munchen, Germany

²Fakultat fur Physik, Ludwig-Maximilians-Universitat Munchen, Scheinerstr. 1, D-81679 Munchen, Germany

³Department of Physics ‘Ettore Pancini’, University of Naples Federico, II, I-80126 Naples, Italy

⁴NASA Goddard Space Flight Center, Greenbelt, MD 20771, USA

⁵SETI Institute, 189 Bernardo Ave, Suite 200, Mountain View, CA 94043, USA

⁶Department of Physics, Astronomy, University of Kansas, 1082 Malott, 1251 Wescoe Hall Dr., Lawrence, KS 66045, USA

⁷Space Telescope Science Institute, 3700 San Martin Drive, Baltimore, MD 21218, USA

⁸Department of Astronomy, University of Florida, Gainesville, FL 32611, USA

⁹Infrared Processing and Analysis Center, Caltech, Pasadena, CA 91125, USA

¹⁰Exoplanets and Stellar Astrophysics Laboratory, Code 667, NASA Goddard Space Flight Center (GSFC), Greenbelt, MD 20771, USA

¹¹Oxford Dynamics, G19, Building R71, RAL, Didcot OX11 0QX, UK

¹²Geoscience Department, University of Aveiro, Campus Santiago, 3810-193, Aveiro, Portugal

¹³School of Science and Engineering, Meisei University, 2-1-1 Hodokubo, Hino, Tokyo 191-0042, Japan

¹⁴Institut de Física d’Altes Energies (IFAE), Barcelona Institute of Science and Technology, E-08193 Barcelona, Spain

¹⁵Citizen Scientist, Planet Patrol Collaboration

¹⁶IATE-OAC, Universidad Nacional de Córdoba-CONICET, Laprida 854, X5000 BGR, Córdoba, Argentina

¹⁷Staples High School, 70 North Ave, Westport, CT 06880, USA

¹⁸Department of Computer Science Brown University, 115 Waterman St, Providence, RI 02906, USA

¹⁹SA Citizen Science Group-Ignited Minds VIPNET Club

Accepted 2022 March 7. Received 2022 March 7; in original form 2022 January 21

ABSTRACT

The *Transiting Exoplanet Survey Satellite* (TESS) has detected thousands of exoplanet candidates since 2018, most of which have yet to be confirmed. A key step in the confirmation process of these candidates is ruling out false positives through vetting. Vetting also eases the burden on follow-up observations, provides input for demographics studies, and facilitates training machine learning algorithms. Here, we present the TESS Triple-9 (TT9) catalog – a uniformly vetted catalog containing dispositions for 999 exoplanet candidates listed on ExoFOP-TESS, known as TESS Objects of Interest (TOIs). The TT9 was produced using the Discovery And Vetting of Exoplanets pipeline, DAVE, and utilizing the power of citizen science as a part of the Planet Patrol project. More than 70 per cent of the TOIs listed in the TT9 pass our diagnostic tests, and are thus marked as true planet candidates. We flagged 144 candidates as false positives, and identified 146 as potential false positives. At the time of writing, the TT9 catalog contains ~ 20 per cent of the entire ExoFOP-TESS TOIs list, demonstrates the synergy between automated tools and citizen science, and represents the first stage of our efforts to vet all TOIs. Our final dispositions and comments are collected in a supplementary table and the DAVE-generated files are publicly available on ExoFOP TESS.

Key words: catalogues – planets and satellites.

1 INTRODUCTION

A plethora of ground- and space-based exoplanet-hunting efforts have contributed to the exponential growth of the number of discovered planets orbiting stars other than our Sun. Prior to 2010,

exoplanet discoveries were mainly based on precise radial velocity curves, e.g. (Mayor & Queloz 1995; Marcy et al. 1998; Lovis et al. 2005; Naef et al. 2010). A paradigm shift in exoplanet discoveries started with NASA’s Kepler mission (Borucki et al. 2008), launched in 2009. This endeavor enabled the scientific community to gather a large exoplanet sample via the photometric transit technique. This mission alone contributed to the confirmation of more than 2700 exoplanets and the discovery of as many candidate exoplanets still

* E-mail: luca.cacciapuoti@eso.org

to be confirmed.¹ The wealth of planet-like signals discovered by photometric surveys will likely grow and expand, thanks to large archival data sets, and ongoing and future planned survey missions, e.g. *Transiting Exoplanet Survey Satellite* (TESS) (Ricker et al. 2015) and the PLANetary Transits and Oscillations (PLATO) of stars (Rauer et al. 2021).

Indeed, since 2018, the TESS space mission has been surveying most of the sky and searching for additional transiting exoplanets. TESS has already identified more than 5000 TESS Object of Interest (TOIs), i.e. candidate exoplanets, and is expected to detect thousands more, e.g. (Barclay, Pepper & Quintana 2018). However, only 199 out of the ~5000 TOIs listed on ExoFOP-TESS have been statistically validated and/or confirmed at the time of writing, according to the NASA Exoplanet Archive. Given that non-planetary astrophysical sources [most notably eclipsing binary stars; see e.g. Ciardi et al. (2018)] and/or systematic effects can often mimic exoplanet transits, revealing the true nature of the remaining TOIs requires ruling out possible false-positive scenarios and/or follow-up observations.

Ideally, the precision radial velocity (PRV) technique, e.g. (Baranne et al. 1996; Pepe et al. 2004), is utilized to confirm the planetary nature of a specific candidate. This is indeed the method that was used to discover the first confirmed exoplanet orbiting a Sun-like star: 51 Pegasi b (Mayor & Queloz 1995). Specifically, the stellar spectrum is obtained at different epochs to detect periodic Doppler shifts of its absorption lines due to the orbit of the star around the centre of mass of the star-planet system. The major downside of the PRV technique is that spectroscopic observations are time-consuming. To be able to detect a planet around a star with the PRV method, two conditions should apply. First, the star has to be sufficiently bright to allow observing its spectrum in a reasonable amount of time and with a sufficient signal-to-noise ratio (SNR). Secondly, planets with short orbital periods facilitate the detection since this allows obtaining complete cycle radial velocity curves in a reasonable amount of observing time. Given the number of exoplanets an all-sky survey like TESS is expected to discover (Barclay et al. 2018), it is unfeasible to obtain PRV observations for every star with a transiting planetary candidate.

Thus, vetting procedures play a critical role in the analysis of exoplanet candidates. First, vetting is needed to ease the burden of ground-based follow-up facilities and to validate planets for which no PRV measurements can be obtained. Secondly, it is fundamental to refine the true population of known exoplanets that underline demographics and population synthesis efforts. Finally, vetting serves as a mean to build a knowledge base for upcoming machine-learning codes that will have the necessary function of validating the stream of new candidates.

A number of pipelines have been developed to validate photometric signals caused by transiting exoplanets, such as ROBOVETTER (Coughlin 2020) and AUTOVETTER (Jenkins et al. 2014). These codes are based on supervised machine learning – a single decision tree for the former and a random forest algorithm for the latter – and have been trained to recognize true planet candidates (PC) based on tens of thousands of human-inspected signals available at the time of development. Other algorithms, like VESPA (Morton 2015) and TRICERATOPS (Giacalone et al. 2021), compute the Bayesian probability that the signal might be a false positive (FP) based on the number of nearby sources (NSs) in TESS field of view, their properties, as well as the shape and strength of the investigated signal. Yet another approach, pioneered by ASTRONET (Shallue & Vander-

burg 2018) for Kepler and exploited by ASTRORAMJET (Olmschenk et al. 2021) for TESS, utilizes a deep learning algorithm known as a Convolutional Neural Network. The code is trained to recognize patterns in light curves and discriminate among classes based on the data alone. Finally, Kostov et al. (2019a) used the Discovery And Vetting of Exoplanets (DAVE) pipeline that tests the candidate signal at both the pixel and light-curve levels mimicking the process that expert human vetters apply. Kostov et al. (2019a) made use of DAVE to uniformly vet 776 K2 candidates and collected the data and dispositions in a catalog hosted on the Kepler Threshold Crossing Event Review Team website. Since then, DAVE has been adapted to TESS data and used to vet a handful of individual PCs, see e.g. Kostov et al. (2019b) and Gilbert et al. (2020).

Here, we present the TESS Triple-9 (TT9) catalog of 999 uniformly vetted exoplanet candidates detected in TESS data. The candidates were identified by the community using the Science Processing Operations Center pipeline (SPOC, Jenkins et al. 2016) and Quick Look Pipeline (QLP, Huang et al. 2020) pipelines, and are listed on ExoFOP-TESS. To create the catalog, we vet the signals employing the DAVE pipeline and citizen science. Specifically, each candidate is analysed through DAVE and inspected by human vetters, and also utilizing auxiliary information as provided by ExoFOP TESS.² This effort has been possible also thanks to the Planet Patrol project (Kostov et al., accepted for publication on PASP), a NASA-led citizen science project hosted on Zooniverse through which a group of citizen scientists interested in validating TESS planets joined our science team. The main goal of Planet Patrol is to evaluate the reliability of DAVE results with the help of volunteers. The outcomes of the classifications have been implemented in DAVE to rule out bad images and compute high-fidelity photocentre statistics. Soon after the launch of the project, several citizen scientists expressed interest in further helping the vetting efforts and, after joining the science team, quickly became proficient vetters. These ‘Superusers’ have been key to the success of this endeavour. The Superusers and the science team members will be referred hereafter as ‘vetters’.

This paper is organized as follows. We present our vetting workflow in Section 2; the details on the citizen science project Planet Patrol are described in Section 3; the TESS Triple-9 catalog is presented in Section 4. Finally, we wrap up the conclusions in Section 5.

2 THE VETTING WORKFLOW

For every TOI listed in our TT9 catalog, we performed a uniform vetting analysis following a workflow that is based on the interpretation of DAVE results using as input the transit ephemeris, duration, and depth as provided by ExoFOP-TESS. Where available, we also evaluate ancillary information that the pipeline does not account for, such as archival data. The workflow proceeds as outlined in the next subsections, it is summarized in Fig. 1, and it is mainly based on products generated by the DAVE pipeline that we describe below.

(i) **PHOTOCENTRE**: this module of DAVE generates the in-transit and the two (before and after the event) out-of-transit images for each transit. Then, it subtracts the in-transit image from the average out-of-transit image to produce a difference image. Finally, it measures the centre-of-light for each difference image by fitting the TESS pixel-response-function and a Gaussian point-spread-function to the image. This is highlighted in Fig. 2 for the case of TIC

¹<https://exoplanetarchive.ipac.caltech.edu>

²<https://exofop.ipac.caltech.edu/tess/>

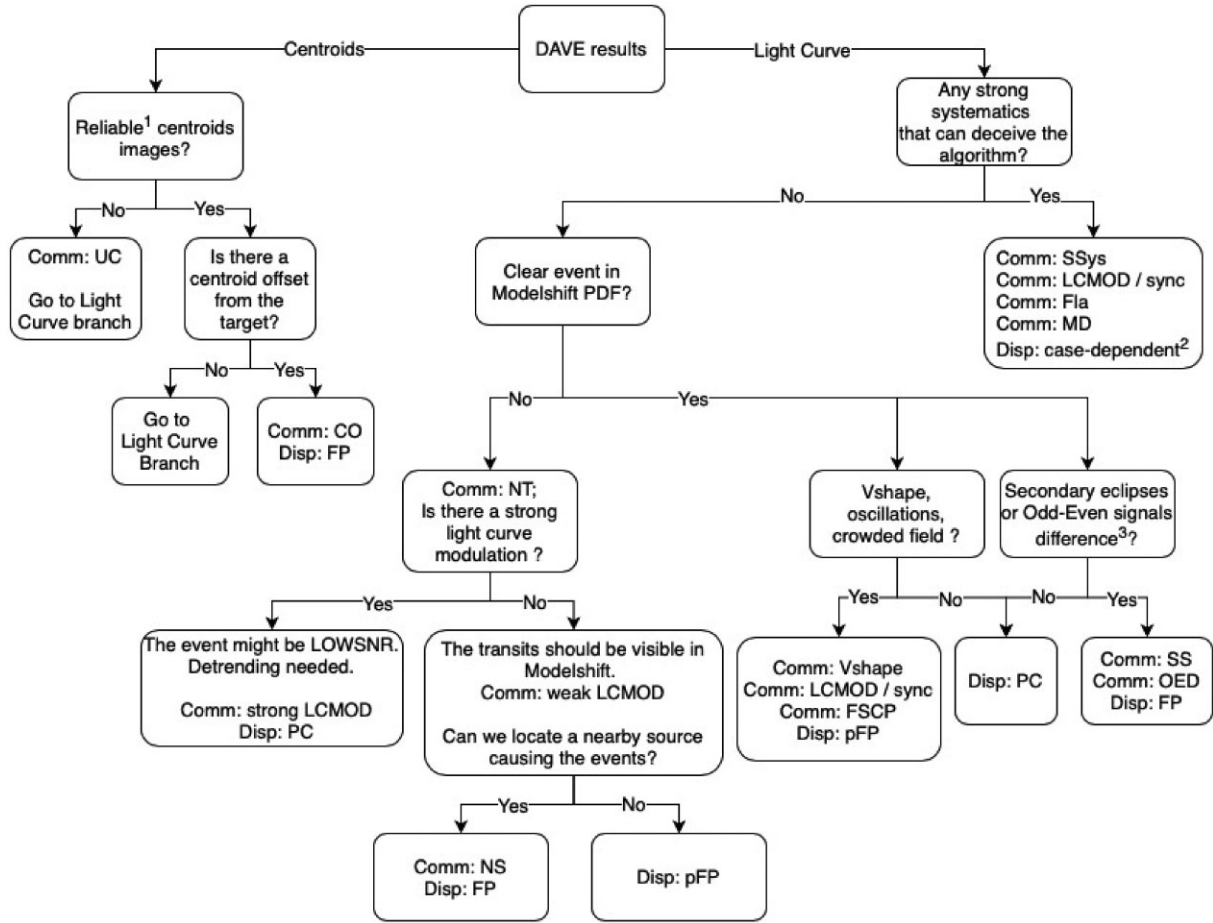


Figure 1. A flow diagram showing the algorithmic process the vetters would go through during the vetting of the TOIs. The workflow starts with the left ‘Centroids’ branch and moves on to the ‘Light Curve’ branch if needed, as explained in Section 2. All of the used abbreviations are shown in Table 1. Footnote¹: centroids are considered reliable if no other field bright variable source is present. Footnote²: the mentioned features could make it difficult to interpret the nature of the signal without jeopardizing its true planetary nature *a priori*. Footnote³: Given that these secondary eclipses and/or odd-even differences are not caused by any irregular feature in the light curve (previously inspected).

43647325, where a fainter field star is present a few pixels above and to the right of the target (upper right panel). This field star is, however, not present in the difference image, demonstrating that it is not varying in brightness during the detected transit events. The measured photocentres are on-target (black star; TIC 43647325), confirming that it is the source of the detected transits. The overall photocentre (red circle) is calculated by averaging over the individual photocentres (red dots) corresponding to each detected transit as examined in the previous step (see Fig. 2). See Kostov et al. (2019a) for further details.

(ii) **MODELSHIFT**: this module of DAVE phase-folds the light curve and convolves it with a trapezoid model using the transit parameters provided on ExoFOP-TESS, thus highlighting light-curve features that resemble the detected transits but occur at orbital phases other than zero. The module is designed to highlight the average of the input primary signals, the average of the odd and even signals, and the most prominent secondary, tertiary, and positive features. The results of the module are summarized in an automatically generated PDF file (see Fig. A1). See Kostov et al. (2019a) for further details.

(iii) **LOMB-SCARGLE**: DAVE runs a Lomb–Scargle (LS) periodogram (Lomb 1976; Scargle 1982) and generates a PDF file showing both the light-curve phase-folded on the period of the inspected signal and the best-fitting LS period (see Figs 1, 3). This test is performed to

help the vetter check whether the modulations occur on the same (or half) period of the candidate signal. In such cases, the vetter might comment for potential beaming, ellipsoidal, and/or reflections effects that might indicate a binary star system, see (Morris & Naftilan 1993; Faigler & Mazeh 2011; Shporer 2017). Performing this test is the reason we opt out of applying custom detrending of the light curves.

(iv) **Summary**: DAVE produces a summary PDF file that contains the full light curve, a zoom-in of each transit in the light curve, the photocentre module images and the LS result.

Besides DAVE results, the vetters consulted stellar catalogs, such as SIMBAD (Wenger et al. 2000) and Gaia EDR3 (Gaia Collaboration 2021), to keep track of the field stars in *TESS* images. This is critical to assess whether known nearby field stars could potentially be the true source of the observed *TESS* signals. Accompanying DAVE products and our final dispositions, we kept track of any noticeable feature for each TOI by means of comments. The details of these are listed in Table 1.

2.1 Photocentre analysis

As a first step, the vetter would start with the critical problem of pinpointing the true source of the transit-like events. Individual *TESS* pixels cover a sky-projected area of 21×21 arcsec². This often means

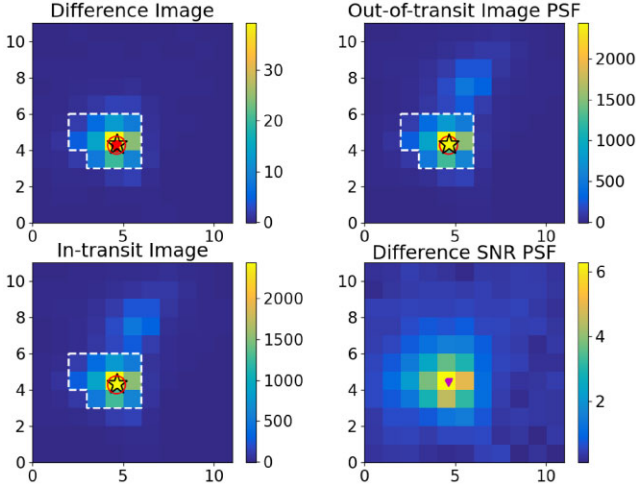


Figure 2. DAVE photocentre analysis for TIC 43647325. Upper right: the average out-of-transit *TESS* image. The white contour represents the pixels used to extract the light curve, the black star represents the catalog position of the target, the purple triangle represents the measured average out-of-transit photocentre, and the red circle represents the measured difference image photocentre; lower left: the average in-transit image; upper left: difference image highlighting the location of the source (black star symbol) varying in brightness during the detected transits. The colourbar units are in electrons per second (e^-/s). Taking into account DAVE results as a whole, this TOI has been marked as a PC.

that one or more field stars fall in the same pixel as the target or in the aperture used to extract the light curve. First, the vetter would inspect stellar charts and catalogs to evaluate whether any known sources fall within the aperture. Next, they would check if these sources are bright enough to cause the transit-like signal in the light curve based on the measured transit depth and on the magnitude difference between the target and the source. For every target, we considered a threshold Δmag such that only field stars with a magnitude within this limit could cause a signal with the same depth of the one under consideration. In cases for which one or more such sources are identified, the final disposition for the TOI is accompanied by the comment Field Star in Central Pixels (FSCP). This procedure is complementary to the photocentre inspection, during which the vetter would examine the *TESS* difference images generated by DAVE and identify the true source of the signal (see Fig. 2).

If the difference images present a photocentre shift away from the target, the candidate signal is considered a FP since the signal is coming from a different star and the disposition is accompanied by the comment centroid offset (CO). If the corresponding difference images show a well-defined group of pixels centred on the target, the candidate signal would pass the centroid analysis. There are cases for which the centroid difference images are difficult to interpret due to artefacts, stray-light, or low SNR. When this was observed to be the case, vetters would comment with unreliable centroids (UC). We note that small exoplanets could produce low-SNR signal in *TESS* data which would also result in poor photocentre images. If the light curves did not show any other red flag, we would flag the poor quality of the measured photocentres but still label the signal as planet candidates (PC).

2.2 Light-curve analysis

Once the measured photocentres have been analysed, we inspect the full light curve for every available sector. It is worth noting that

we use *ELEANOR* ‘corrected flux’ light curves (Feinstein et al. 2019) without any processing such as custom detrending or removal of any data point. This visual inspection is necessary to assess whether prominent systematics could make DAVE automated dispositions unreliable. During our work, unreliable detections were mostly observed when using *TESS* Full Frame Images-extracted light curves. Since DAVE uses un-detrended data by design, this step is also critical in situations where strong stellar variability is present. The variability can throw off the evaluation process of some features such as the depth difference between odd and even signals (see Fig. 3). The light-curve variability is also quantified with a LS periodogram and a phase-folded light curve is provided as a part of a summary PDF for every *TESS* Input Catalog (TIC; as in Fig. 3).

Thus, the full light curve and the LS PDFs aid the vetters in evaluating the *MODELSHIFT* result while taking into account potential irregular behaviour in the light curve. This step of the analysis results in comments about the light curve and the signals added to the final disposition. Typical comments used in this phase are LCMOD, Fla, MD, WE, and SSys (see Table 1 for the details). The next step is to inspect the *MODELSHIFT* PDF, in which the folded light curve and the primary and second-order features are highlighted.

The vetter would inspect the DAVE evaluations on top of the PDF (see Fig. 4, A1), listed in a table where numbers in red indicate potential issues for the respective candidate signal [see Kostov et al. (2019a) for details]. This table could highlight significant additional eclipses, odd-even depth difference, or even positive spikes. However, vetters have been trained to evaluate the issues raised by *MODELSHIFT* based on what they have seen in the previous step, i.e. the full light-curve inspection. For example, when the light curves present a modulation, the vetters do not automatically interpret an odd-even difference flagged by DAVE as a strong indicator of a FP. Instead, the vetters would point out the necessity to detrend the light curve to obtain a final disposition based on the consistency of the depth of consecutive signals. Again, during the *MODELSHIFT* inspection, vetters could identify features with the comments listed in Table 1.

2.3 Final dispositions and comments

For each target, at least three vetters, plus one science team member, have performed a complete and thorough vetting as described, in an effort to minimize the subjectivity of the process by mediating among different dispositions. The results of this effort are described in Section 4. The final dispositions presented in our catalog are as follows:

- (i) a PC is a TOI that passes all of the described vetting tests.
- (ii) a FP is a TOI that does not pass one or more tests. It is one with unambiguous non-planetary nature.
- (iii) a potential FP (pFP) is a TOI for which multiple issues have been identified by DAVE, by the vetters, or by both – yet we cannot securely rule it out as a clear FP because, for example, the SNR is low, or the signal is coming from a pixel containing comparably bright multiple sources.

To clarify, an example of a pFP might be a TOI presenting a potential secondary eclipse in an otherwise flat light curve (pSS; defined as an additional eclipse that does not stand out beyond the blue 1σ noise level lines in the *MODELSHIFT* PDF, see Fig. 4, A2). A second example is a candidate signal that exhibits prominent V-shaped eclipses and light-curve modulations (LCMOD) coherent with the orbital period of the TOI yet no significant secondary eclipses or CO were found. Furthermore, a candidate for which there are no discernible transit-like features in the light curve is also flagged

Table 1. List of abbreviations used during the vetting process. The first part of the table shows the final disposition abbreviation. The second half displays the general comments that have been used to support the disposition. A (p) is used next to certain comments and means *potential*. The human vetters would add a (p) in case DAVE did not automatically flag the feature due to lack of statistical significance.

Abbreviation	Meaning	Description
Disposition		
PC	Planet Candidate	A TOI that passed all vetting tests.
(p)FP	False Positive	A TOI that does not (fully) pass the vetting tests.
Comments		
(p)SS	Significant Secondary	A statistically significant secondary is highlighted by the <code>MODELSHIFT</code> module. A secondary eclipse is typical of an eclipsing binary star.
(p)CO	Centroid Offset	A significant photocentre shift is detected. This indicates that the target star is not the source of the investigated signal.
UC	Unreliable Centroids	A centroid image is considered unreliable if stray light, bright field stars or low SNR cause the difference image to be too noisy for proper photocentre measurements.
(p)OED	Odd-Even Difference	A statistically significant difference between odd and even eclipses is highlighted by the <code>MODELSHIFT</code> module and/or the vetters, indicating an eclipsing binary star.
(p)Vshape	V-shape	The shape of the signal is not U-shaped, as expected from a typical transit, but rather V-shaped. A transiting planet (usually with $R < R_{\text{star}}$) is expected to produce a sharp ingress, a flat bottom, and a sharp egress. In contrast, an eclipsing star (usually with $R \sim R_{\text{star}}$) often produces gradual ingress and egress.
TD	Too Deep	For a given stellar radius, the deeper the eclipse, the larger the eclipser. As the deepest confirmed exoplanet eclipses range between 3 and 4 per cent ¹ , e.g. (Noyes et al. 2008; Triaud et al. 2013), we flag signals with depth greater than 2.5 per cent. We note that we do not use TD as the only indicator for a (p)FP as the stellar radius provided in by ExoFOP-TESS might be under/overestimated.
FSCP	Field Star in Central Pixel	TESS pixels cover a sky-projected area of 21×21 arcsec ² each. This means that other sources might fall within the same pixel of the target and be the true source of the signal.
LCMOD	Light-Curve MODulation	Oscillations in the light curve due to intrinsic and/or rotational variability (potentially due to pulsations or spots) that are not synchronized with the orbital period. These can be produced by either the target itself or by a nearby field star that falls in the aperture used to extract the light curve. Such light curves are generally not indicative of a potential FP.
sync	Synchronous Modulations	Light-curve variations synchronized with the TOI orbital period (or half) are common features of variable binary stars. For example, stars in binary systems with small orbital separations can be deformed into ellipsoids due to tidal effects. The light curves of these systems can show sinusoidal oscillations on half of the eclipses period due to changes in the light-emitting area of the components along the orbital phase, (Shporer 2017). Such light curves are generally indicative of a potential FP.
EB	Eclipsing Binary	An eclipsing binary system.
HPMS	High Proper Motion Star	A high proper motion star as listed on SIMBAD. ^a
SSys	Strong Systematics	The long-cadence <code>ELEANOR</code> light curve displays strong artifacts.
Fla	Flares	<code>TESS</code> light curve shows potential flaring events. These are sharp rises in flux followed by an exponential decay.
NT	No Transit	The <code>ELEANOR</code> light curve does not show noticeable transit-like signals for QLP-detected TOIs. The <code>MODELSHIFT</code> module flags the candidate due to the low statistical significance of the expected signal.
NS	Nearby Source	We identify a nearby source that is the true source of the signal. This has been achieved using the <code>ELEANOR.PIXEL_BY_PIXEL()</code> function, as explained in Section 4.2.
MD	Momentum Dump	<code>TESS</code> thruster-firing-induced artefact in the light curve.
LOWSNR	Low Signal to Noise Ratio	The SNR of the expected transits is too low for reliable vetting.

^a <http://simbad.u-strasbg.fr/simbad/>

as a pFP. In contrast to pFPs, an FP disposition is a representative of a clear secondary eclipse on the same period of the primary, odd-even transit depth differences, or a photocentre shift during the detected transits. Along with these dispositions, we also provide comments on any other noticeable features using the abbreviations listed in Table 1.

3 CITIZEN SCIENTISTS-LED DEVELOPMENT OF ADDITIONAL VETTING TOOLS AND RESOURCES

The Planet Patrol citizens scientists have not only been fundamental to the vetting process, but have also been responsible for major contributions to the presentation and visualization of the results.

LC led a team of volunteers to produce an introductory Video Tutorial hosted on YouTube, in order to help lower the bar for further involvement in the vetting process by the wider community. The

video introduces the key concepts about the search for transiting exoplanets and describes the vetting process through examples.

HADL has produced video recordings of all of our meetings, which can serve as further introduction to vetting, as well as informal tutorials, recommendations, guidance, resources, etc. for newcomers. The recordings are posted on YouTube. If there is sufficient interest in the community, we will migrate these recordings to a dedicated repository.

Yet another project that emerged from the superuser group (led by RS, a student at Staples High School) is the development of a custom web-based interface designed to streamline the vetting process – in essence, a dedicated vetting portal. Currently, we are using Google Sheets to collect the dispositions from each vetter for each target, which involves manual input of thousands of entries (e.g. using the abbreviations listed in Table 1 plus free text). This is a slow and sometimes cumbersome process prone to errors. To address this issue, we are transitioning to a custom Graphical User

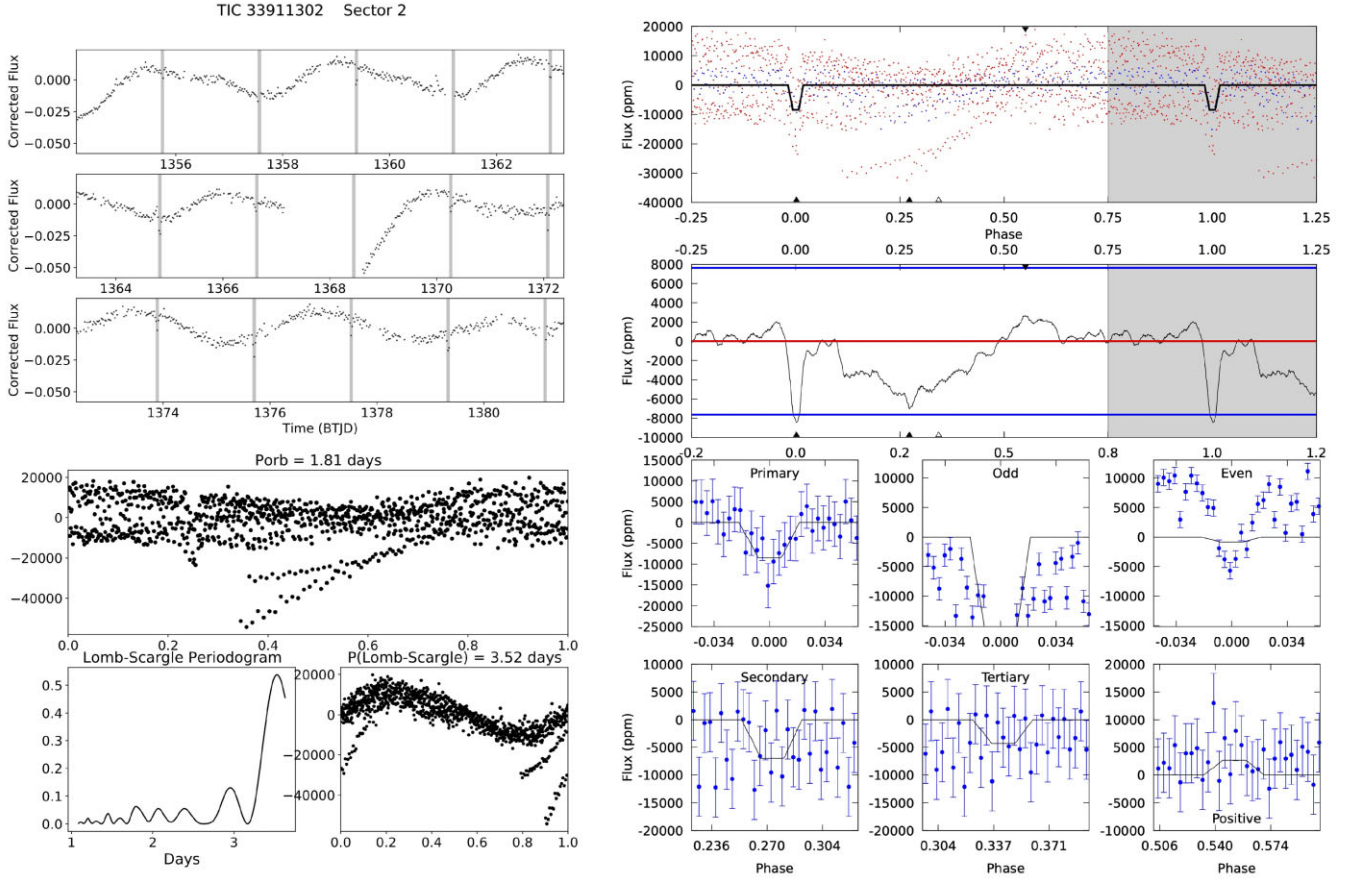


Figure 3. Prominent stellar variability seen in the light curve of TIC 33911302 (upper left panel). The variability is quantified by DAVE through an LS analysis and provided to the vetter as a phase-folded light curve (lower left panels). Such light-curve variability can result in nominal FP disposition by the `MODELSHIFT` module (right-hand panel) due to measured odd-even difference – but can be overruled by the vetter as an incorrect automated disposition. The first panel of the `MODELSHIFT` shows the phase-folded light curve along with the best-fitting transit model (black line); the second panel of the `MODELSHIFT` plot shows the same as the upper panel but the light curve is convolved with the transit model; the lower panels show zoom-ins on the primary and secondary events (as labelled), the odd and even primary events, as well as any tertiary or positive events. The uppermost table displays the significance of the aforementioned features, see Kostov et al. (2019a) for the details. This TOI has been labelled as a PC because the variability is not reminiscent of beaming, reflection, and/or ellipsoidal effects. The observed oscillations could be due to stellar variability of the target itself or of another source that falls within the group of pixels used to extract the light curve. There is no hint of a secondary eclipse standing out of the light-curve noise. We note that since the stellar variability for this target is not coherent with the orbital period, the ‘Vshape’ flag alone is not sufficient to indicate a TOI as a pFP.

Interface which allows user-friendly drop-down menus, multiple-choice answers, free text, automated uploading of targets that still need to be vetted, etc. For completeness, we briefly describe the development of the vetting portal below.

The website was written in Typescript React, is hosted by Heroku at Planet Patrol Website, and stores data in an IBM Cloud; the source code can be found at GitHub. While designing the website, it was important to be mindful of the workflow that vetters were accustomed to. For example, the vetting portal has to (i) present information in a condensed and easy-to-navigate layout; (ii) allow users to find relevant information regarding each target, including the corresponding ExoFOP-TESS link and the PDF files produced by DAVE in PDF format; (iii) let users write dispositions on each target, giving them as much freedom in their comments while requiring a machine-readable format; and (iv) facilitate effective analysis of user dispositions. The portal expanded the user experience by including options to easily sort the table by parameters, finding targets by number of dispositions, and by providing direct links to the vetting PDFs produced by DAVE (using the Google Drive API to automatically search for the relevant document). Also, the portal

offers drop-down menus to input dispositions, buttons with the predefined comments of Table 1 and free-text input – all of which can be accessed in machine-readable format. Lastly, the new website includes features that automatically highlight targets that still need to be vetted by the user, the dispositions, and comments of other users, as well as the final group dispositions.

3.1 Lessons learned

As a part of this work, we kept record of aspects that could be useful for similar citizen science efforts. For the benefit of the community, here we share our experience.

(1) Zooniverse talk board is a convenient method for engaging with the volunteers. We tried to respond to every question as quickly as possible and also provided a Google Form for them to exploit their interest (if any) and ask to join the group of SuperUsers.

(2) Only about a third of the volunteers who signed up for further involvement in the project were active and participated in the weekly

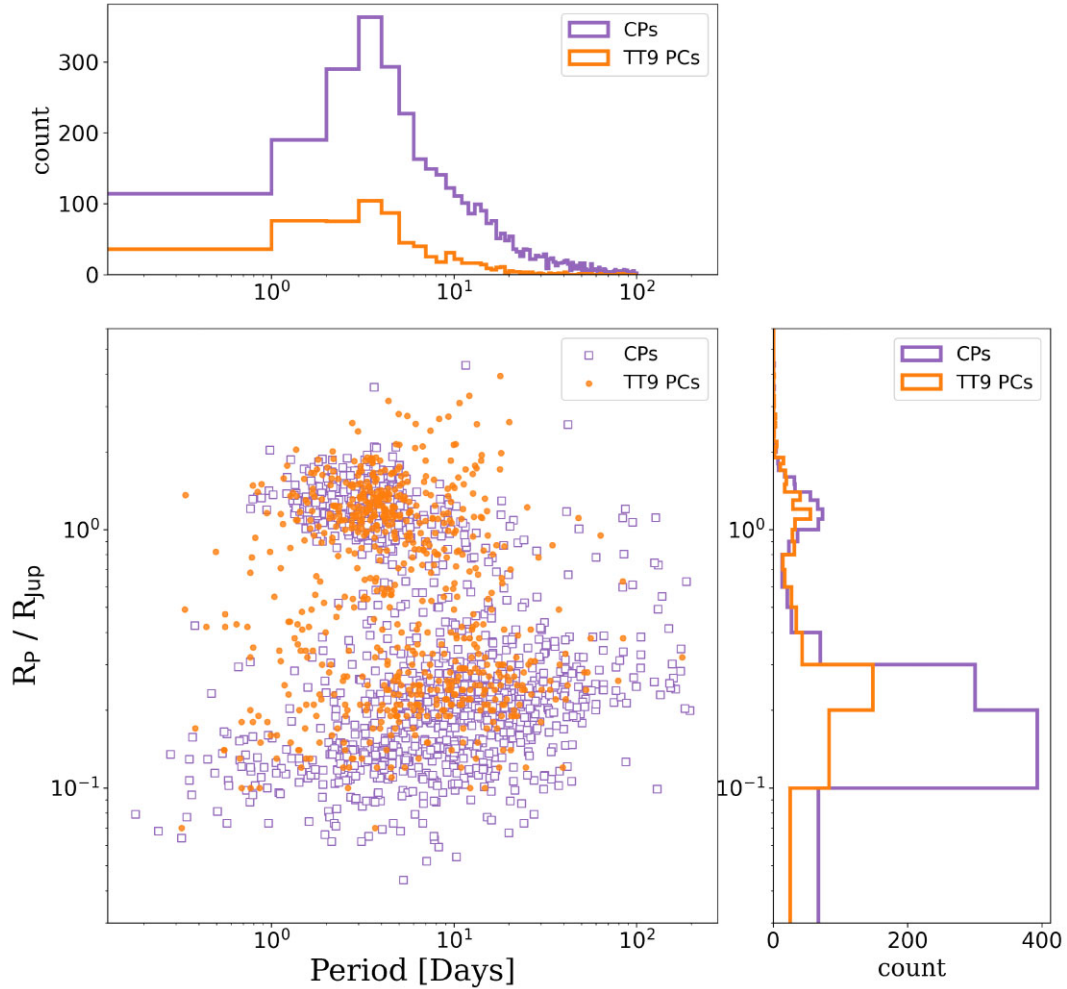


Figure 4. Comparison between the 709 planet candidates in the TT9 catalog (orange circles) with a subset of the entirety of confirmed exoplanets (purple squares). We report confirmed exoplanets discovered via the precise radial velocities and transits techniques with a period lower than 200 d for clarity.

meetings. We suspect part of the reason is the time difference, as outlined below.

(3) Regular interactions between the science team and the SuperUsers were vital for the success of the effort. For offline discussions, we used a dedicated Google Group and a Slack channel; both worked well. For live discussions, we used Google Meet. However, scheduling a weekly meeting that worked for people spread across the world was difficult and we believe this would be an issue for any citizen science project that attract the interest of people worldwide. While the North/South American and European/African time zones could be covered simultaneously from a single location, volunteers from the Asian/Australian time zones were practically left out due to the time difference. One solution to this issue could be to have two separate weekly meetings, led from two locations separated by 12 h.

(4) Keeping a video recording of the meetings provided a convenient catch-up option for SuperUsers who could not participate in the meetings.

(5) An easy-to-use, intuitive, and comprehensive tutorial is crucial to get volunteers who join further along during the project up to speed in a reasonable time frame. The resources and tools developed as a part of the Planet Patrol project, and the information gathered and synthesized, could be used in the future as such tutorials.

(6) The information provided by ExoFOP-TESS, Gaia, MAST, Simbad, Vizier, and other publicly available databases was an important contribution for the success of the project. It allowed volunteers to not only gain deeper understanding of the particular target they were vetting but, as a natural consequence, also of general astronomical concepts such as spectroscopic binary stars, parallax, proper motion, SED, etc.

4 THE TESS TRIPLE-9 CATALOG

The TT9 catalog contains half the TOIs listed on ExoFOP TESS as of 2020 October; we plan to present the rest of our vetting analysis in future work. The TOIs have been detected by the SPOC and QLP pipelines using the 2-min and 30-min cadence data. The specifics of these pipelines are presented in Jenkins et al. (2016) and Huang et al. (2020). Our analysis led to the vetting of 709 signals as true planet candidates (PC), i.e. TOIs that have passed all our vetting tests. We identified 144 TOIs as FPs and 146 as pFP. The dispositions have been collected in a table with period of the eclipses, epoch, depth, duration, stellar and TOI estimated radii, the stellar TESS magnitude, and general comments (see Table 2).

Table 2. The final result of our work is a table of dispositions for 999 TOIs. Here, we report an extract of it. For each TOI, we display the TIC identifier of the star, the signal parameters input in DAVE, the radius of the potential transiter, the radius of the star, the *TESS* magnitude of the star, and the final disposition with related comments. The full table is available as an electronic supplement.

TIC ID	Sectors	Epoch (BTJD)	Period (d)	Duration (h)	Depth (ppm)	R_p (R_J)	R_s (R_\odot)	$TESS_{mag}$	Disposition	Comment
1003831	8	2458518.203	1.651 142	0.76	3007	0.49	0.98	10.6701	PC	TOI 564 b
1103432	8	2458519.87	3.727 891	3.87	17864	1.66	1.34	12.8283	pFP	pTD, pVshape, FSCP, pSS
1129033	4	2458410.985	1.360 025	2.16	16381	1.09	0.95	9.62713	PC	WASP-77 A b
1133072	8	2458517.532	0.846 542	2.41	2525	0.15	0.33	12.625	pFP	FSCP, LCMOD, short-P
1449640	5	2458440.434	3.501 75	3.80	14123	1.98	1.70	11.921	FP	SS
1528696	5	2458438.406	0.882 02	0.58	9750	1.50	0.78	13.1686	PC	NGTS-6 b
2758565	2	2458356.031	3.781 92	2.04	15390	2.35	1.17	12.3611	pFP	pSS,TD
4616072	6	2458469.062	4.185 99	2.85	12942	1.70	1.56	12.8893	PC	HATS-45 b
4646810	4	2458416.346	14.490 034	1.59	905	0.23	0.78	8.8723	PC	
4897275	21	2458872.341	16.710 042	5.40	615	0.24	1.09	7.6474	PC	HPMS
5109298	7	2458491.797	1.6221	2.43	2310	0.94	2.22	10.6698	FP	Vshape, CO
5772442	7	2458492.502	1.105 78	1.87	673	0.67	2.62	10.351	FP	NS

4.1 Planet candidates

Of the 709 TOIs marked as PCs in TT9, 146 have already been confirmed according to ExoFOP *TESS*. The largest among these are hot Jupiters discovered by ground-based projects like the Wide Angle Search for Planets (WASP; Pollacco et al. 2006), the Hungarian-made Automated Telescope Network project (Bakos et al. 2013), the XO effort (McCullough et al. 2005), the Qatar Exoplanet Survey (Alsubai et al. 2013), the Kilodegree Extremely Little Telescope survey (Pepper, Gould & Depoy 2004), and the Next Generation Transit Survey (Wheatley et al. 2018). The smallest planets are instead discoveries of space-based missions: CoRoT (Catala et al. 1995), Kepler (Borucki et al. 2008), K2 (Howard 2015), and *TESS*.

The most common comments for our PCs are ‘FSCP’ (81 times), ‘LCMOD’ (77 times), and ‘V-shaped signal’ (Vshape, 55 times). The first is expected since *TESS* cameras pixels cover a 21×21 arcsec area on the sky, resulting in a frequent blend of multiple sources. The second can either be caused by modulation of the target star itself or from sources that fall within the aperture used to extract the light curve. Finally, a V-shaped transit is not a conclusive proof against the planetary nature of a transiter, but it suggests that the dimensions of the two celestial objects at play are comparable. This is expected to happen for binary star systems more than a planet–star pair due to geometrical reasons even though large hot Jupiters with grazing transits have also been shown to produce this type of signal, e.g. (Smalley et al. 2011; Mancini et al. 2014; Bento et al. 2017). We note that we label as PC also 4 TOIs for which we do not see clear transits in the light curves, which instead display strong modulations. In these cases the modulations could be strong enough to hide weak transit signals that could appear after detrending, which we do not perform. Hence, we keep these as PCs since a signal might have been actually detected if the data were properly detrended and comment with ‘NT’ and ‘strong LCMOD’.

The final PC yield of the TT9 catalog is shown in Fig. 4, in terms of orbital period and planet radius, and also compared to a subset of confirmed exoplanets. We only display confirmed exoplanets that have been discovered via the radial velocity and transit photometry techniques, with periods shorter than 200 d for clarity (3884 out of the total 4935 confirmed exoplanets listed on the NASA Exoplanet Archive, as of mid-2022 January). A depression in the number of planet candidates is observed for the TT9 PCs, as well as for the confirmed exoplanets when $0.3R_J < R < 1.0R_J$.

4.2 False positives

A total of 144 TOIs in our catalog have been flagged as FPs. The most common reason is a significant photocentre shift during transit – 76 targets – while secondary eclipses have been registered for 48 candidate signals. In six cases, the poor quality of the light curve might have deceived the detection pipeline that locked on to features like gaps in the sectors, momentum dump (MD) spikes, or other systematics (TICs 24364065, 47384844, 101929303, 150247134, 169177766, and 198384408). Only two TOIs show significant odd-even differences between consecutive transits (TIC 9033144 and TIC 230086768). LCMODs are present in 32 cases. Of these, eight display modulations coherent with the orbital period (TICs 2758565, 93963408, 96246348, 97158538, 141663460, 141663464, 198457103, and 233720539). We kept track of such modulations for the following reasons. First, in some cases they could be triggering the detection pipelines and be mistaken for candidate planets. Secondly, LCMODs coherent with the orbital period of the transiting exoplanet candidate can be indicative of a short-period eclipsing binary. Finally, even though the detected modulation is not the deciding factor for the FP disposition, we include it for the sake of completeness.

We note that in some cases more than one FP red flags were raised.

Another frequent source of FPs we identified is non-detections of QLP-based PCs in *ELEANOR* light curves. As mentioned above, our analysis is based on the latter because vetting transiting PCs detected by one pipeline but using light curves produced by another is highly valuable as it provides an independent set of tests and and confirmations (e.g. Kostov et al. 2019a)³. Specifically, DAVE uses *ELEANOR*-generated ‘Corrected Flux’ light curves to perform its tests on the TOIs for which only FFI data are available. For some targets in our catalog, the *ELEANOR* light curves do not show obvious transit signals at the ephemeris provided by ExoFOP-*TESS*. In these cases, the vetters would label them as being pFPs rather than certain FPs. This is mainly because the apparent lack of transit signals in *ELEANOR* data can be caused by differences between the QLP pipeline (through which the signals were discovered) and the

³We note that the QLP light curves were not publicly available at the start of this project. As we aim for consistency and uniformity instead of completeness, we continued our analysis with *ELEANOR* data even after the QLP light curves were uploaded to MAST.

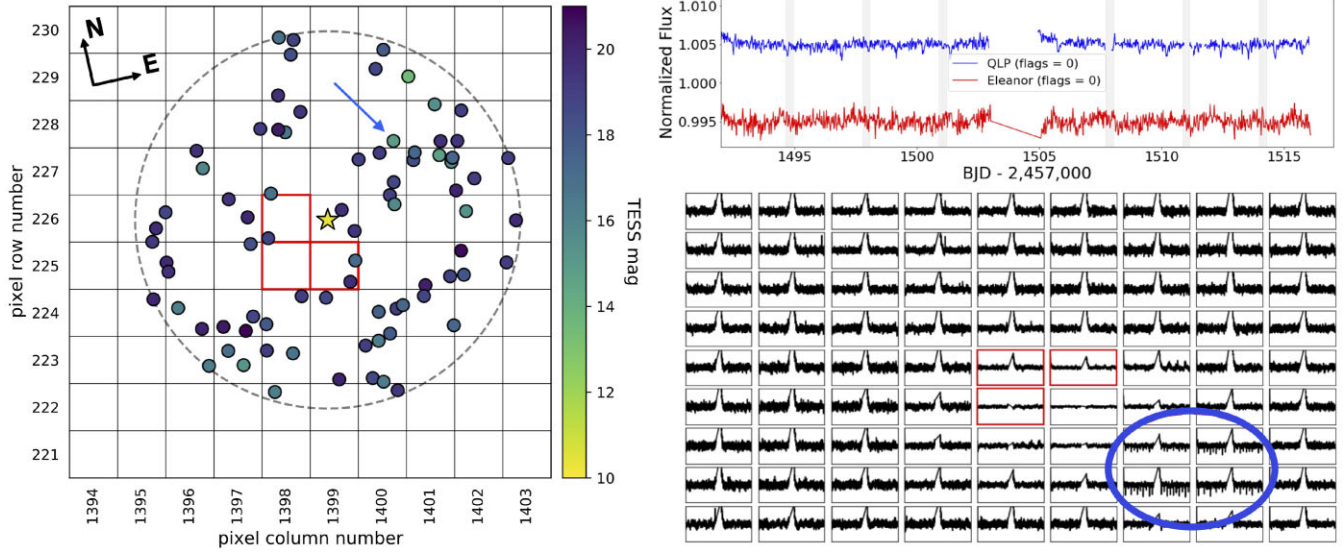


Figure 5. The left-hand panel shows the 10×10 TESS pixels centred on the target (yellow star), the field stars brighter than $T_{\text{mag}} = 21$ mag (dots) within a 4-pixel radius, the ELEANOR aperture (red solid outline), and the source of the signals detected in QLP (blue-dashed arrow). The colourbar shows the TESS magnitude of the field sources. The image has been created using the code TRICERATOPS (Giacalone et al. 2021). Upper right panel: TESS sector 7 QLP (blue) and ELEANOR (red) light curves for TIC 5772442. While the transits of the TOI are clear with a period of approximately 2.5 d in the QLP light curve, no sign of them is present in the ELEANOR-extracted data. In this case, we use the ELEANOR pixel-by-pixel light curves (lower right panel) to find that the signal is coming from a NS (blue outline in upper right panel) while the light curve extracted for the target using the ELEANOR aperture (red solid outline in middle panel) is flat. This TOI is thus a FP. We note that (i) the ELEANOR aperture does not include the target star; and (ii) the lower panel is flipped along the horizontal axis compared to the lower right panel.

ELEANOR pipeline (through which we vet them). Altogether, there are 53 such ‘No Transit’ (NT) cases. We have already mentioned why four of them have been labelled as PC in the previous subsection.

We note that because there is no apparent transit-like signal for these NT TOIs in ELEANOR data, we cannot perform a photocentre analysis. Thus to analyse them and produce a final disposition, we visually inspected the corresponding light curves using the `ELEANOR_PIXEL_BY_PIXEL()` routine. This function allows the user to inspect the light curves of single pixels within the downloaded TESS pixel cutout. Specifically, we would compare the ELEANOR aperture used to extract the light curve to the single pixels light curves. The fact that ELEANOR uses a different aperture optimization algorithm implies that the final light curve is extracted from a different set of pixels and might be different with respect to the QLP one.

Indeed, we found 14 (out of the 53 NT cases) for which the QLP-detected signal is coming from a NS instead of the target under investigation and we finally label these as FPs. We report an example of this case in Fig. 5.

Finally, we note that six confirmed planets have been labelled in TT9 as FPs due to the presence of significant secondary eclipses – despite the fact that these are confirmed hot Jupiters. These dispositions, however, are based on our definition of an FP, i.e. a candidate exhibiting clear secondary eclipses (see Fig. A3). Thus even though we are aware that these ‘secondary eclipses’ are in fact planetary occultations, for consistency we flag the six TOIs as FPs (see also Table 3 and Section 4.4).

4.3 Potential false positives

As described in Section 2, we have labelled as pFP 146 TOIs for which we could not confirm the suspected non-planetary nature yet identified a number of potential issues. For these TOIs, we identified various combinations of: V-shape morphology, ultra-short periods, potential secondary eclipses, potential photocentre offset,

Table 3. Confirmed planets in the TT9 catalog for which our vetting efforts identify prominent secondary eclipses. According to our vetting workflow, these planets had to be flagged as FPs in TT9 because we do not have sufficient information to distinguish between an occultation and a secondary eclipse.

TIC	Name	~Depth (ppm)	Comments
16740101	KELT9-b	600	Occ
22529346	WASP-121 b	200	Occ
86396382	WASP-12 b	400	FSCP, Occ
100100827	WASP-18 b	300	Occ
129979528	WASP-33 b	500	LCMOD, Occ
158324245	KOI-13 b	400	Occ

field stars in the same pixel of the target that are bright enough to produce the detected signals as contamination, and/or coherent LCMODs as commonly seen in short-period eclipsing binaries. We reported examples of pFPs that could be due to unresolved background sources in Fig. 6 and Fig. A2. Programs such as TFOP⁴ could clear these cases, thanks to higher-resolution photometric measurements, spectroscopic observations, high-resolution imaging, or precise radial velocity measurements. Specifically, we identified 49 cases showing potential photocentre offset and 32 cases for which a potential secondary eclipse has been identified. A total of 69 pFPs display LCMODs, of which 33 are synchronous with the eclipses (sync). Finally, 35 TOIs show NT event but, as opposed to the FP cases, we could not identify NSs showing the expected eclipses.

In some cases, more than one of these red flags have been raised by the vetters.

⁴TESS Follow-Up Observing Programs.

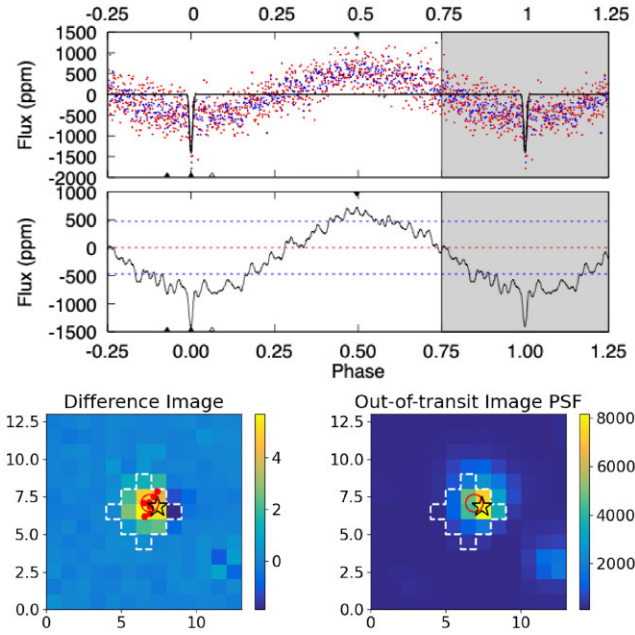


Figure 6. An example of pFP: TIC 97158538. The upper panel presents a portion of the `MODELSHIFT` results. Here, one can see that the TOI presents LCMODs coherent with eclipses. The lower panels display the out-of-transit *TESS* image (lower right) and the difference image (lower left) between in- and out-of-transit frames. The colourbars show units of electrons per second (e^-/s). Given the large scatter in the measured photocentres, likely caused by the light-curve variability, we note a potential, sub-pixel centroids offset.

4.4 Confirmed planets

For consistency, we vet targets independent of any prior knowledge of the system, and regardless of their current disposition on ExoFOP. Some of them are listed as confirmed planets and were added to our catalog for completeness. Our analysis of confirmed planets supports the planetary nature interpretation of 140 of them and flagged 6 as FPs. The reason for the latter dispositions is as follows.

When large, close-in planets pass behind their host star along the line of sight with the observer, a secondary dip in the light curve can be observed due to the occultation of the light reflected and/or emitted by the planet. Occultations allow direct measurement of the planet's radiation (hence its effective temperature) and helps constrain the planet's orbital eccentricity. Our analysis highlighted this kind of signal as a FP indicator since the event is effectively identical to a secondary eclipse. We find such occultations in the light curves of six of the confirmed planets in the TT9, and we label these signals as FPs since we vetted every TOI without prior knowledge of its current status. An example is shown in Fig. A3. We report the TICs of these candidates, along with the approximate depth of the secondary eclipse as seen in *TESS* bandpass (600–1000 nm), in Table 3. For completeness, we also point out the other disposition comments for these targets where applicable.

4.5 Potential new signals

During the analysis presented above, the vetters picked up new signals not previously reported on ExoFOP *TESS*. We inspect these one by one and check whether they could be identified with known systematic effects, such as MD, i.e. artefacts caused by *TESS* thruster firings. This can be done by comparing the signals to the registered

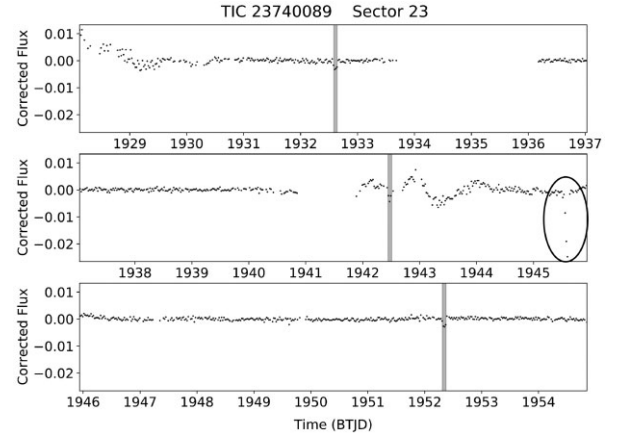


Figure 7. Long-cadence light curve of TIC 23740089. The highlighted signals are the events detected by the QLP pipeline that we vet with DAVE. An additional eclipse is observed at BTJD 1945.5. If this were the primary eclipse of a circular binary system, such that the detected TOI is in fact secondary eclipses, we would have to observe the same type of feature at approximately 1935.6 and 1955.3. Neither time was observed due to a data gap and the finite time range of the *TESS* sector so we cannot confirm this hypothesis.

MDs events in *TESS* Data Releases.⁵ These new signals are as follows.

An additional eclipse has been flagged for TIC 23740089, located at BTJD 1945.5 in sector 23. This TIC hosts what we have labelled as a PC with a $0.59 R_J$ candidate orbiting a $1.14 R_\odot$ star in 9.8 d. The additional, deeper (> 2 per cent) eclipse is only observed once between transits two and three (see Fig. 7). According to *TESS* Data Release Notes for sector 23, this event does not correspond to a thruster firing event. The separation between the TOI and this additional signal is such that we could be missing the same deeper eclipse event after transit number one due to a data gap and the one after transit number three due to the finite duration of the sector. Thus, the available ELEANOR-extracted *TESS* data does not have sufficient coverage to assess whether this event might indicate a binary star and we labelled the target as a PC with an extra eclipse. *TESS* will observe again the target between 2022 February 26 and 2022 April 22 which might allow to clear this specific case.

We detected two additional events in the light curve of TIC 74534430 at approximately 1539.6 and 1545.0 BTJD (in sector 8 and 9) that do not fall on any reported MD events. These events are shallower and shorter than the TOI transits, which is labelled in TT9 as a PC with an orbital period of 18 d and radius of $0.19 R_J$, orbiting a $0.61 R_\odot$ star. The target has been observed by *TESS* in sectors 8, 9, 35, and 36.

We also observed additional, non-periodic events in the light curve of TIC 128501004 in sector 16, the only one available for the target. No additional *TESS* observations are scheduled for this star. Two different deep events have been noticed in the light curve at approximately 1747.9 and 1748.2 (BTJD), neither of which corresponds to a MD event. TIC 128501004 is a $1.1 R_\odot$ star hosting a $0.18 R_J$ object (labelled as a PC in TT9) with an orbital period of 0.8 d. However, taking into account the additional events, this candidate could be a triple star system which will require further observations to be confirmed.

⁵https://archive.stsci.edu/tess/tess_drn.html

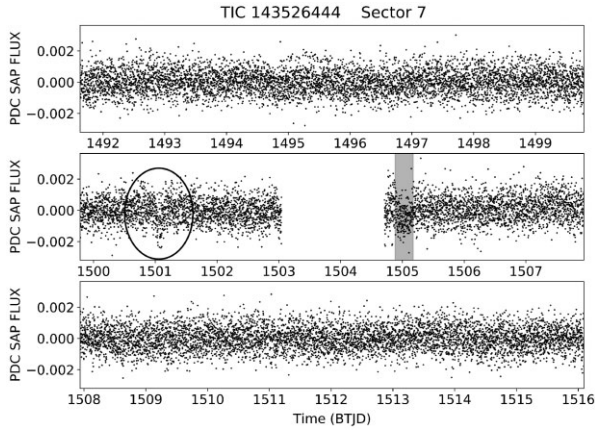


Figure 8. Short-cadence sector 7 light curve of TIC 143526444. The vertical grey band highlights the transit of the candidate in the ExoFOP TOIs catalog. The additional event at BTJD 1501 (black oval) is likely caused by a momentum dump as reported in *TESS* data release notes. We do not find any similar event in the other available sectors.

An additional event is present in the light curve of TIC 143526444 in sector 7 (see Fig. 8). The target is a $3.5 R_{\odot}$ star hosting a $0.9 R_J$ PC with an orbital period of 15.3 d. The event is at time 1501 (BTJD) where an MD event has been registered and reported in *TESS* Data Release Notes #9. Thus, we reject this extra event as an artefact.

Finally, a potential new candidate has been observed in the *TESS* sector 4 light curve of TIC 100990000 at an epoch of approximately 1425 (BTJD). This transit-like feature is a single event within the four available *TESS* sectors (3, 4, 30, and 31) and has a duration of roughly 6 h which is consistent with a long period. If confirmed, this candidate would be the outermost planet in a system with other two planets (Earth- and Super-Earth-sized) orbiting a G-type star in 4.04 and 9.57 d, respectively. The estimated radius of the new candidate is $2.7 R_{\oplus}$. The characterization of this system is being carried out in Cacciapuoti et al., submitted. We note that we have recently learned that this candidate has also been uploaded on ExoFOP-*TESS* as TIC 100990000.03 by a citizen scientist of the Planet Hunters *TESS* project (Eisner et al. 2021).

5 CONCLUSIONS

We presented the TT9 catalog, containing 999 uniformly vetted transiting exoplanet candidates from *TESS*. We marked 709 TOIs as bona fide PCs, of which 146 are confirmed exoplanets. Additionally, 144 TOIs were flagged as FPs due to photocentre motion during transit, significant secondary eclipses, and/or LCMODs indicative of eclipsing binary stars. Finally, 146 TOIs were labelled as pFPs due to too many potential issues to be passed as PCs yet no definitive evidence to be ruled out as clear FPs.

The TT9 catalog is provided to the community in a table format (see Table 2) which provides our final dispositions, along with additional comments for each TOI. For completeness, the table also includes the transit ephemeris, depth, and duration, and the *TESS* magnitude. The table is available as supplementary material along this paper. The DAVE generated MODELSHIFT and summary PDFs, as well as the centroid images for each TOI in each sector have been made available on ExoFOP *TESS* at the webpages of each TOI in the "Files" section as well as on the Planet Patrol website. This work presents the first stage of our effort to vet all TOIs listed on ExoFOP-*TESS* using DAVE and citizen science. Our

results provide an independent analysis of known TOIs and could be used to prioritize follow-up observations. The dispositions provided in the TT9 catalog can be also utilized as input for demographic studies of transiting exoplanets from *TESS* or as a training set for machine learning algorithms aimed at automating vetting efforts.

ACKNOWLEDGEMENTS

This research has made use of the NASA Exoplanet Archive, which is operated by the California Institute of Technology, under contract with the National Aeronautics and Space Administration under the Exoplanet Exploration Program.

We acknowledge the use of public *TESS* Alert data from the pipelines at the *TESS* Science Office and at the *TESS* Science Processing Operations Center (SPOC) and from the Massachusetts Institute of Technology Quick Look Pipeline (QLP).

This research has made use of the Exoplanet Follow-up Observation Program website, which is operated by the California Institute of Technology, under contract with the National Aeronautics and Space Administration under the Exoplanet Exploration Program.

This publication uses data generated via the Zooniverse.org platform, development of which is funded by generous support, including a Global Impact Award from Google, and by a grant from the Alfred P. Sloan Foundation.

We thank the referee for the insightful comments which helped improve the manuscript.

Software: DAVE (Kostov et al. 2019a), ELEANOR (Feinstein et al. 2019), QLP (Huang et al. 2020).

DATA AVAILABILITY

The data underlying this article will be shared on reasonable request to the corresponding author.

REFERENCES

- Alsubai K. A. et al., 2013, *Acta Astron.*, 63, 465
- Bakos G. Á. et al., 2013, *PASP*, 125, 154
- Baranne A. et al., 1996, *A&AS*, 119, 373
- Barclay T., Pepper J., Quintana E. V., 2018, *ApJS*, 239, 2
- Bento J. et al., 2017, *MNRAS*, 468, 835
- Borucki W. et al., 2008, in Cambridge University Press, , Sun Y.-S., Ferraz-Mello S., Zhou J.-L., eds, *Exoplanets: Detection, Formation and Dynamics*, Cambridge University Press, p. 17
- Catala C. et al., 1995, in Ulrich R. K., Rhodes E. J. J., Dappen W., eds, *ASP Conf. Ser.*, Vol. 76, GONG 1994. Helio- and Astro-Seismology from the Earth and Space. Astron. Soc. Pac., San Francisco, p. 426
- Ciardi D. R., Pepper J., Colon K., Kane S. R., Astrophysical Community W. I. f. t., 2018, preprint ([arXiv:1810.08689](https://arxiv.org/abs/1810.08689))
- Coughlin J. L., 2020, *Astrophysics Source Code Library*, record (ascl:2012.006)
- Eisner N. L. et al., 2021, *MNRAS*, 501, 4669
- Faigler S., Mazeh T., 2011, *MNRAS*, 415, 3921
- Feinstein A. D. et al., 2019, *Astrophysics Source Code Library*, record (ascl:1904.022)
- Gaia Collaboration, 2021, *A&A*, 649, A1
- Giacalone S. et al., 2021, *AJ*, 161, 24
- Gilbert E. A. et al., 2020, *AJ*, 160, 116
- Howard A., 2015, *Discovery and Characterization of Small Planets from the K2 Mission*. NASA ADAP Proposal
- Huang C. X. et al., 2020, *Res. Notes Am. Astron. Soc.*, 4, 204

Jenkins J. M., McCauliff S. D., Catanzarite J., Twicken J. D., Burke C. J., Campbell J., Seader S., 2014, in *American Astronomical Society Meeting Abstracts*, Vol. 223. p. 206.02

Jenkins J. M. et al., 2016, in Chiozzi G., Guzman J. C., eds, *SPIE Conf. Ser.*, Vol. 9913, *Software and Cyberinfrastructure for Astronomy IV*. SPIE, Bellingham, p. 99133E

Kostov V. B. et al., 2019a, *AJ*, 157, 124

Kostov V. B. et al., 2019b, *AJ*, 158, 32

Lomb N. R., 1976, *Ap&SS*, 39, 447

Lovis C. et al., 2005, *A&A*, 437, 1121

Mancini L. et al., 2014, *A&A*, 568, A127

Marcy G. W., Butler R. P., Vogt S. S., Fischer D., Lissauer J. J., 1998, *ApJ*, 505, L147

Mayor M., Queloz D., 1995, *Nature*, 378, 355

McCullough P. R., Stys J. E., Valenti J. A., Fleming S. W., Janes K. A., Heasley J. N., 2005, *PASP*, 117, 783

Morris S. L., Naftilan S. A., 1993, *ApJ*, 419, 344

Morton T. D., 2015, *Astrophysics Source Code Library*, record (ascl:1503.011)

Naef D. et al., 2010, *A&A*, 523, A15

Noyes R. W. et al., 2008, *ApJ*, 673, L79

Olmschenk G. et al., 2021, *AJ*, 161, 273

Pepe F. et al., 2004, *A&A*, 423, 385

Pepper J., Gould A., Depoy D. L., 2004, in Holt S. S., Deming D., eds, *AIP Conf. Ser.*, Vol. 713, *The Search for Other Worlds*. Am. Inst. Phys., New York, p. 185

Pollacco D. L. et al., 2006, *PASP*, 118, 1407

Rauer H. et al., 2021, in *European Planetary Science Congress*. p. EPSC2021–90

Ricker G. R. et al., 2015, *J. Astron. Telesc. Instrum. Syst.*, 1, 014003

Scargle J. D., 1982, *ApJ*, 263, 835

Shallue C. J., Vanderburg A., 2018, *AJ*, 155, 94

Shporer A., 2017, *PASP*, 129, 072001

Smalley B. et al., 2011, *A&A*, 526, A130

Triaud A. H. M. J. et al., 2013, *A&A*, 551, A80

Wenger M. et al., 2000, *A&AS*, 143, 9

Wheatley P. J. et al., 2018, *MNRAS*, 475, 4476

SUPPORTING INFORMATION

Supplementary data are available at *MNRAS* online.

TT9.csv

Table 2. The final result of our work is a table of dispositions for 999 TOIs.

Please note: Oxford University Press is not responsible for the content or functionality of any supporting materials supplied by the authors. Any queries (other than missing material) should be directed to the corresponding author for the article.

APPENDIX A: MODELSHIFT FIGURES

In this appendix, we display the examples of DAVE MODELSHIFT PDF products that have served as examples during the explanation of the general vetting workflow (Section 2) and of the reasons behind the TT9 dispositions (Section 4).

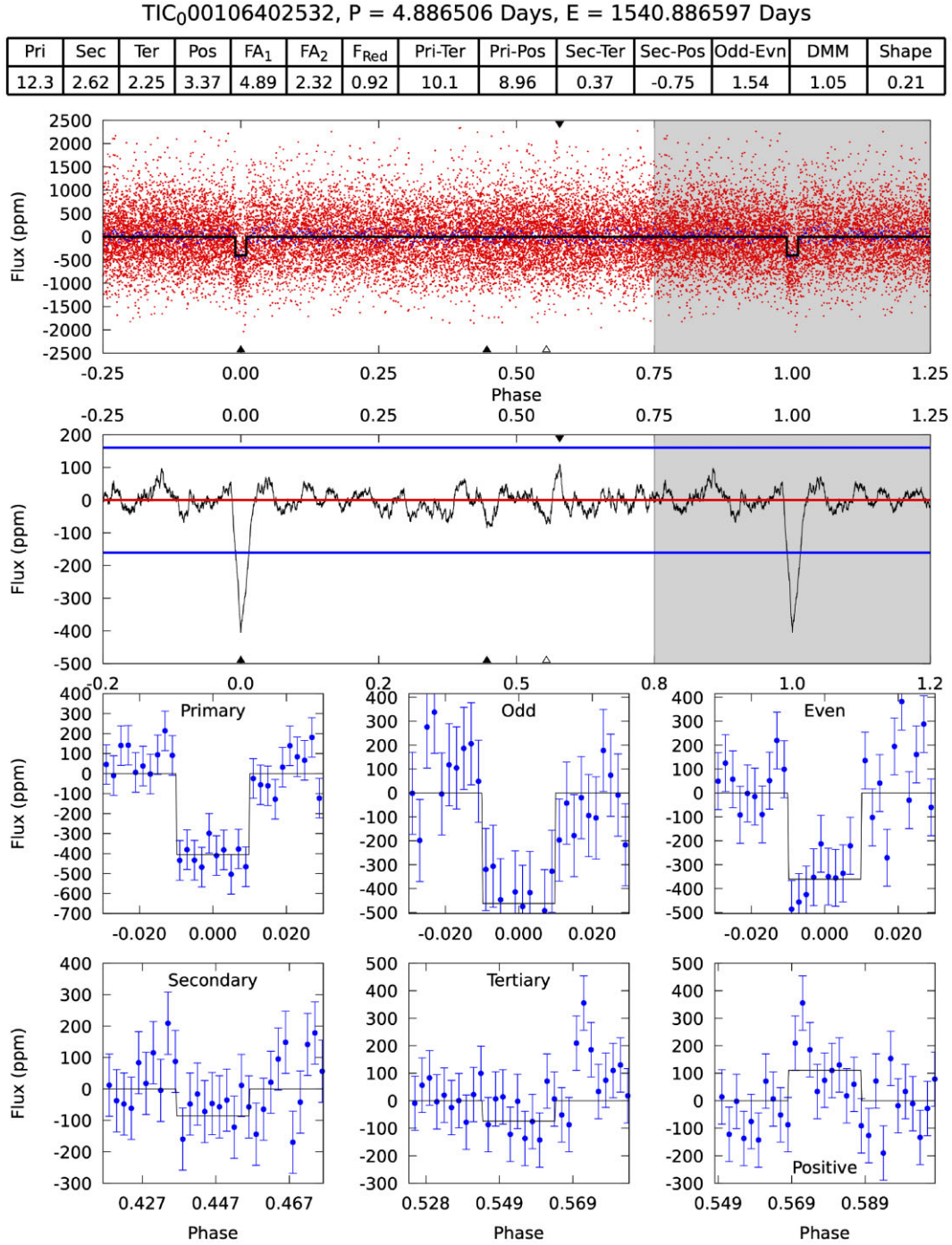


Figure A1. An example of DAVEMODELSHIFT PDF for TIC 106402532 (sector 9). No issues of potential concern have been raised by either DAVE or the vetters for this TOI. Considering the photocentre analysis as well, this TOI is labelled as a bona-fide planet candidate (PC) in the TESS Triple-9 catalog.

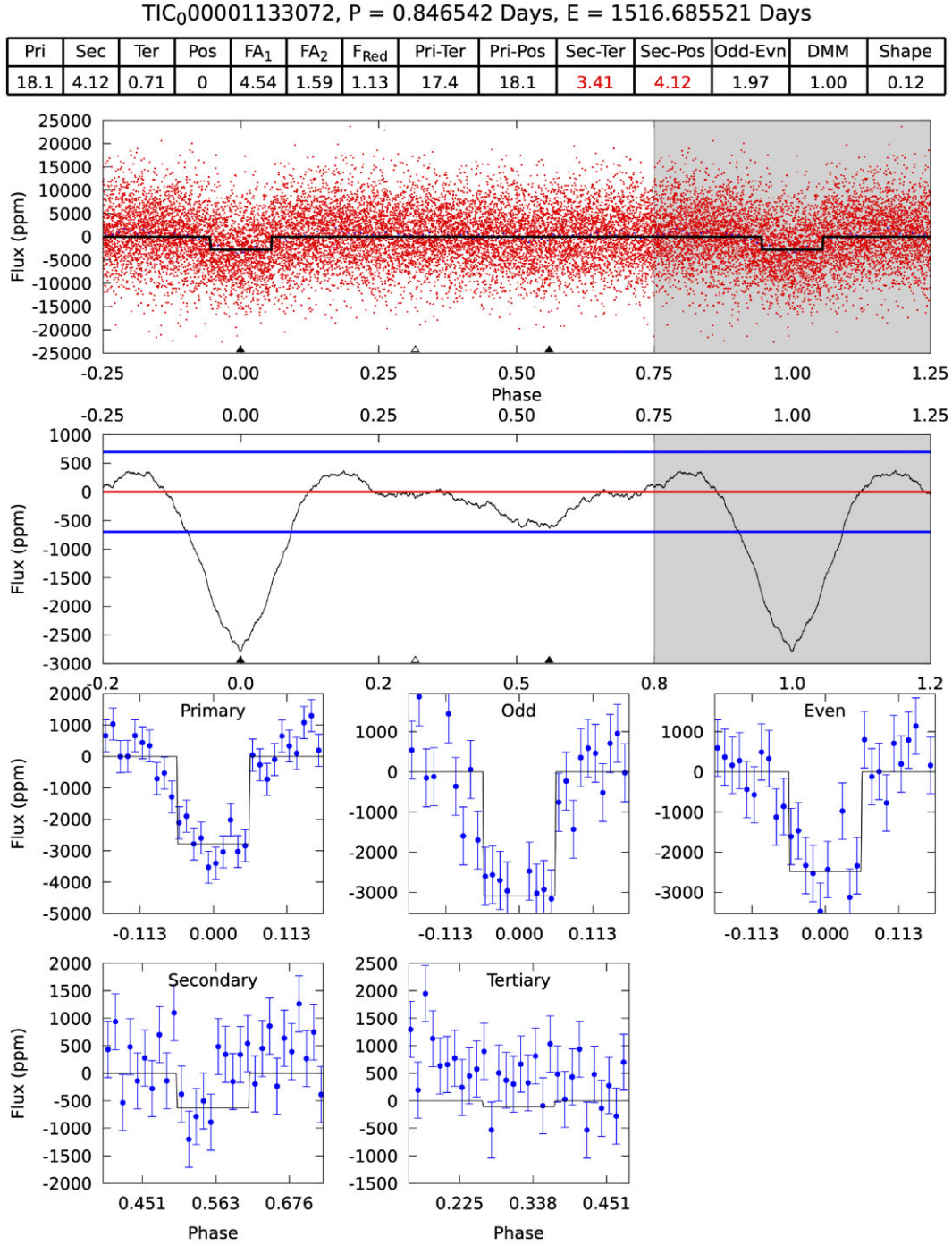


Figure A2. MODELSHIFT PDF for TIC 1133072 (sector 8). The second panel from top (the phase-folded light curve convolved with the transit model) shows a light-curve reminiscent of the modulations typical for β Lyrae-type binary stars, where the primary and secondary eclipses do not have sharp ingress and egress. Given the low SNR, the short orbital period, the V-shaped eclipses, and the potential secondary eclipse near phase 0.5 (note that it is not flagged as significant by DAVE), we flag the target as a pFP.

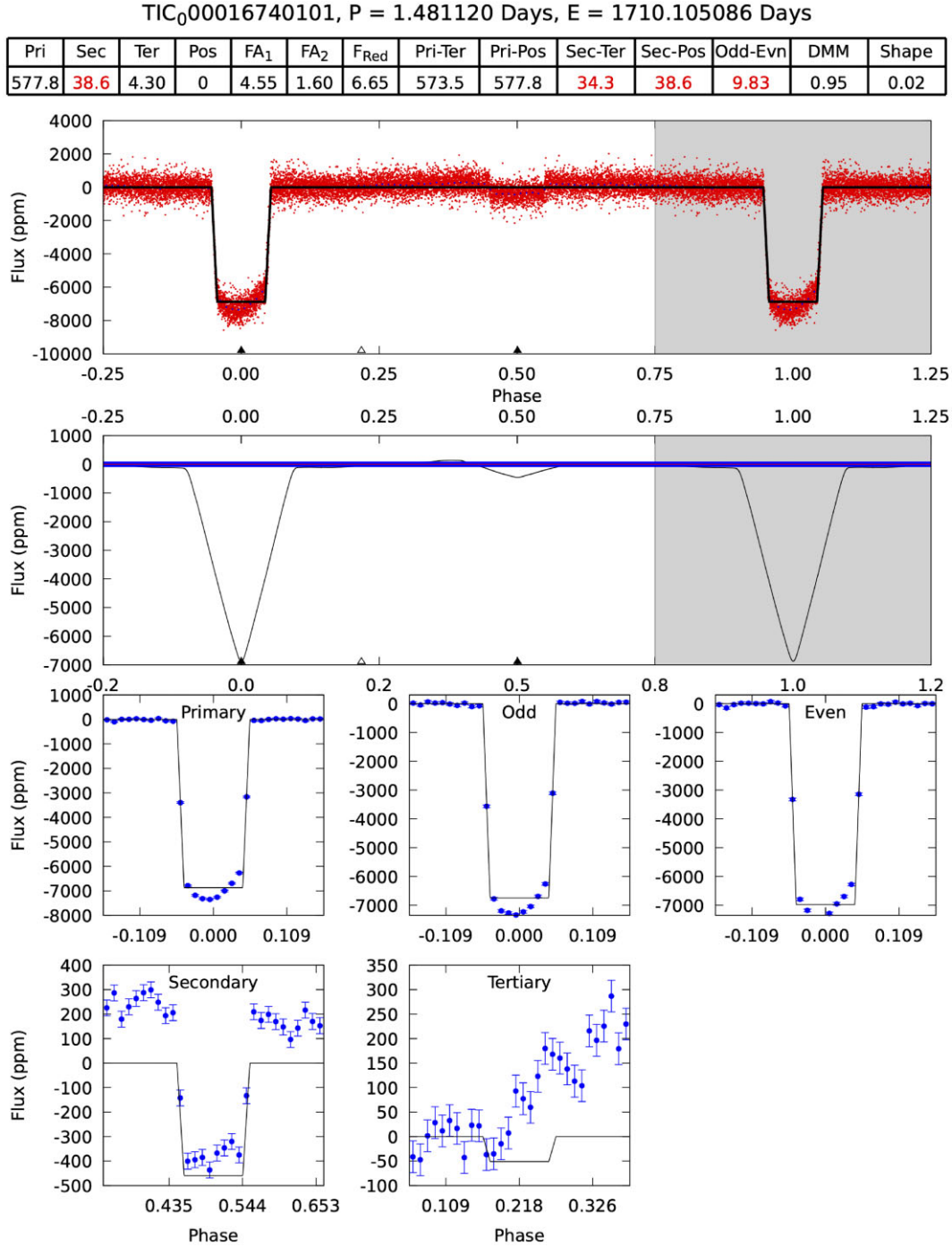


Figure A3. The phase-folded light curve for TIC 16740101, also known as KELT-9 b. A secondary eclipse on the same period of the input signal is clear in DAVE MODELSHIFT result. The secondary is due to the occultation of the bright side of the planet when it orbits behind the star along *TESS* line of sight. Based on DAVE results only, for consistency we label this TOI as FP due to the significant secondary eclipses.

This paper has been typeset from a \LaTeX file prepared by the author.